

Optimization of Energy-Constrained IRS-NOMA Using a Complex Circle Manifold Approach

Mahmoud AlaaEldin, *Student Member, IEEE*, Emad Alsusa, *Senior Member, IEEE*, Karim G. Seddik, *Senior Member, IEEE*, Constantinos B. Papadias, *Fellow, IEEE*, and Mohammad Al-Jarrah, *Student Member, IEEE*

Abstract—This work investigates the performance of intelligent reflective surfaces (IRSs) assisted uplink non-orthogonal multiple access (NOMA) in energy-constrained networks. Specifically, we formulate and solve two optimization problems, one for minimizing the users' sum transmit power and another for maximizing the energy efficiency (EE) of the system. The two problems are solved by jointly optimizing the users' transmit powers and the passive beamforming coefficients at the IRS reflectors subject to the users' individual uplink rate constraints. A novel algorithm is developed to optimize the IRS passive beamforming coefficients by optimizing the objective function over the *complex circle manifold* (CCM), exploiting the manifold optimization technique. The proposed manifold optimization-based solution is bench-marked against the rather *standard* semi-definite relaxation method (SDR). The results show that the manifold optimization-based algorithm achieves significantly better performance for both transmit power minimization and EE maximization problems at a computational complexity lower than the SDR approach. The results also reveal that IRS-NOMA is superior to the orthogonal multiple access (OMA) counterpart only when the users' target achievable rate requirements are relatively high.

Index Terms—Non-orthogonal multiple access, intelligent reflective surfaces, energy-efficient networks, manifold optimization, complex circle manifold, semi-definite relaxation.

I. INTRODUCTION

Recently, intelligent reflective surfaces (IRS) have emerged as a new technology in the wireless research community [1]–[4]. IRS is a planar surface that consists of a large number of adjustable and low-cost passive reflecting elements which can reflect the incident signals after applying certain amplitudes and phase shifts. The IRS technology is attractive as it can be an effective solution for improving the spectral and energy efficiency of wireless networks [5]. The core characteristic of IRSs lie in their ability to *engineer* the wireless channel between the transmitter and receiver to realize different design purposes like signal strengthening and interference mitigation.

Moreover, non-orthogonal multiple access (NOMA) has been considered as one of the key techniques that can

Mahmoud AlaaEldin, Emad Alsusa, and Mohammad Al-Jarrah are with the Electrical and Electronic Engineering Department, University of Manchester, Manchester, UK M13 9PL (e-mail: mahmoud.alaeldin@manchester.ac.uk; e.alsusa@manchester.ac.uk; mohammad.al-jarrah@manchester.ac.uk).

Karim G. Seddik is with the Department of Electronics and Communications Engineering, American University in Cairo, Cairo, Egypt 11835 (e-mail: kseddik@aucegypt.edu).

Constantinos B. Papadias is with the Research, Technology and Innovation Network (RTIN), Alba, The American College of Greece, 153 42 Athens, Greece, and also with the Department of Electronic Systems, Aalborg University, 9220 Aalborg, Denmark (e-mail: cpapadias@acg.edu).

significantly enhance both the spectral efficiency (SE) and energy efficiency (EE) of wireless communication networks [6]–[8]. Unlike its orthogonal multiple access (OMA) counterpart, NOMA can serve multiple users using the same frequency/time/code resources, where successive interference cancellation (SIC) can be used at the receiver to decode the different signals [8], [9]. The superiority of NOMA over OMA has been thoroughly investigated in the literature [10]. Motivated by the benefits of both IRS and NOMA technologies, we aim to provide an extensive study on integrating IRS with uplink NOMA. The aim of this study is to minimize the power consumption of battery-based nodes and to maximize EE of the system, while satisfying the quality-of-service (QoS) requirements of each node.

A. Related Work

IRS passive beamforming has been extensively studied in the literature during the past few years. For example, in [11], the authors studied the application of IRS in a single cell scenario with a multi-antenna base station (BS) and multiple single-antenna users. They developed alternation minimization algorithms to minimize the total transmit power at the BS; they used a semi-definite relaxation (SDR)-based optimization approach to design the passive beamforming at the IRS. The authors in [12] proposed efficient algorithms to maximize the EE of IRS assisted downlink communication systems with a multi-antenna BS serving multi-antenna users. More specifically, they developed efficient algorithms based on alternation maximization, gradient descent, and sequential fractional programming to jointly optimize the transmit power allocation at the BS and the IRS phase shifts. IRS has also been used in the literature to boost the performance of simultaneous wireless information and power transfer (SWIPT) systems [13]. In [14], the authors also applied IRS to enhance the energy harvesting performance of SWIPT systems, where a multi-antenna BS simultaneously transmits information and energy to several receivers. In [15], the joint design of a transmit beamforming matrix at the BS and the IRS reflecting coefficients was investigated using deep reinforcement learning (DRL). The authors in [16] studied the use of IRS in an uplink multi-user scenario to optimize the spatial multiplexing performance when a linear receiver is used. Other applications of the IRS include unmanned aerial vehicles (UAVs) communications; for example, the capacity of IRS assisted UAVs communications was analyzed in [17] considering the effect of imperfect phase

knowledge. IRS has also been considered in other applications such as physical layer security for covert communications [18], physical layer network coding [19] and wireless mesh back-hauling [20]. Given such a wide range of applications, IRS is seen as a key enabling technology for the six generation (6G) wireless networks [21].

Prior works have also investigated the integration of IRS in NOMA networks. In [22], the authors designed an IRS assisted downlink NOMA system, where orthogonal beams are generated at the BS using the spatial directions of the near users' channels, then the cell edge users are served on those beams along with the near users using NOMA. The authors in [23] evaluated the performance of IRS assisted power domain NOMA by deriving closed-form expressions for the best-case and worst-case of the outage probability and ergodic rate of the prioritized user. In [24], the rate performance of IRS assisted downlink NOMA was optimized by maximizing the minimum decoding signal-to-interference-plus-noise-ratio (SINR) of all the users to ensure fairness among users. The authors leveraged the block coordinate descent technique and SDR to jointly optimize the NOMA power allocation and IRS phase shifts. In [25], the authors investigated downlink multiple-input single-output IRS assisted NOMA systems, where a multi-antenna BS sends information to multiple single-antenna users. To maximize the sum rate of all users, they used alternation optimization, successive convex approximation, and sequential rank-one relaxation approaches to jointly optimize active beamforming at the BS and passive beamforming at the IRS. In [26], the EE of an IRS assisted downlink NOMA system was maximized by jointly optimizing the transmit beamforming at the BS and passive beamforming at the IRS using an SDR-based optimization technique. In [27], the authors analyzed the error rate performance of IRS assisted downlink NOMA by deriving an approximate expression for the pairwise error probability assuming imperfect SIC. In [28], the authors used dual-polarized IRS to enhance the performance of dual-polarized downlink massive MIMO based NOMA, which allows the BS to multiplex groups of users in the polarization domain. In [29], the authors investigated achieving secure communication for IRS assisted NOMA using artificial jamming sent by a multi-antenna BS along with the NOMA signal. The transmit beamforming, the jamming vector, and the IRS reflecting coefficients were optimized to maximize the sum rate of the users under certain QoS requirements. The authors in [30] considered an IRS assisted uplink NOMA, where the objective was to maximize the sum rate of all the users under individual QoS and power constraints. The authors used alternation maximization and SDR to jointly optimize the users' transmit powers and IRS reflecting coefficients.

B. Motivations and Contributions

In this paper, we consider the IRS assisted uplink NOMA system shown in Fig. 1, where multiple single-antenna users transmit data to the BS using NOMA. We study two main problems, namely, the total users' transmit power minimization and the system's EE maximization. Although some works investigated IRS assisted NOMA, to the best of our knowledge,

no existing work has addressed the total transmit power minimization and system's EE maximization for uplink NOMA systems. These two problems are important for next-generation wireless networks where reducing power consumption, or raising the energy efficiency of the network, is a major concern. In both problems, we use the iterative alternating optimization algorithm to jointly optimize the uplink NOMA transmit powers of the users and the passive beamforming (phase shifts) at the IRS, under minimum QoS constraints for the users. In each iteration of the alternating optimization algorithm, the power allocation problem of the users is solved given the IRS passive beamforming coefficients; then, the IRS coefficients are optimized using the obtained transmit power vector of the users. To solve the IRS passive beamforming sub-problem in each iteration, we devise two different approaches to calculate the IRS reflecting coefficients. Then we compare these against each other. The first approach is based on the SDR technique, while the second one uses manifold optimization.

Surprisingly, the simulation results show that the performance of the proposed manifold optimization-based approach is far superior to the SDR one. Therefore, devising a manifold optimization-based algorithm to solve the passive beamforming sub-problem at the IRS is a key finding of this paper since it provides a huge performance gain when compared to the SDR based approach that is widely used in the IRS assisted NOMA literature, as presented in the related works subsection. The manifold optimization approach beats the SDR based approach in both the total transmit power minimization and the system's EE maximization problems. Although the IRS assisted uplink NOMA system was firstly considered in [30], our work in this paper is different in multiple aspects. Firstly, we study the total transmit power minimization and the EE maximization problems; however, the work in [30] considered the sum-rate maximization problem of the users. Secondly, unlike [30] in which the direct user-BS links were ignored to simplify the system model and algorithm design, we consider the more general scenario where the direct links are considered. Thirdly and most importantly, we devise a very efficient algorithm based on manifold optimization to optimize the IRS reflecting coefficients and compare it against the SDR based solution. However, existing NOMA works focus only on the SDR based algorithms which we prove not to be efficient for solving the considered problems in this paper. Additionally, we propose solutions to the sum transmit power minimization and the EE maximization of the IRS assisted uplink OMA system to compare against the IRS assisted NOMA system. Interestingly, the results show that the performance of the IRS-NOMA system outperforms the IRS-OMA system when the minimum target uplink rate constraints of the users are high. However, the situation is reversed when low minimum uplink rate constraints are required. The contributions of this work are summarized as follows:

- We solve the total transmit power minimization and the EE maximization problems for the IRS assisted uplink NOMA system. Based on the proposed framework, we formulate a joint design for optimizing the users' transmit powers and the IRS phase shifts for each of the two con-

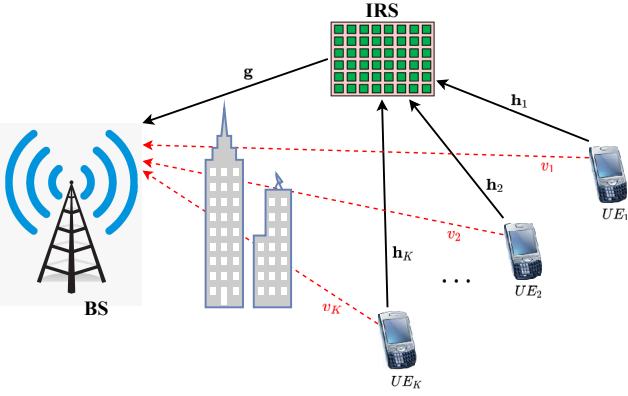


Figure 1: IRS assisted NOMA uplink system model

sidered problems using alternating optimization, subject to minimum user rate constraints and constraints on the IRS reflecting coefficients.

- To solve the IRS passive beamforming design sub-problem, we devise a novel manifold optimization-based approach. In contrast to the SDR approach, the proposed manifold optimization-based algorithm can obtain a locally optimal solution that adheres to the unit-modulus constraints of the IRS reflecting coefficients.
- We show that the proposed manifold optimization-based approach can achieve a huge performance gain for both the transmit power minimization and the EE maximization problems over the SDR based approach that is commonly used in the IRS literature.
- We formulate and solve both the transmit power minimization and EE maximization problems for the IRS assisted uplink NOMA system to compare against the IRS assisted OMA system. The simulation results reveal that NOMA outperforms OMA when the target user rate constraints are high; however, OMA is preferable when the target uplink rates are low. We also illustrate the relation between the transmit power minimization and the EE maximization problems in the simulation results.

The rest of the paper is organized as follows. In Sec. II, the IRS-aided uplink NOMA system model is presented, while in Sec. III, the total transmit power minimization problem is formulated and solved. The EE maximization problem is presented and solved in Sec. IV. In Sec. V, we discuss the IRS assisted uplink OMA system. Finally, simulation results and conclusions are given in Sections VI and VII, respectively.

II. SYSTEM MODEL

As shown in Fig. 1, we consider an IRS-assisted uplink NOMA system in which a group of K single antenna users transmit data symbols to a single antenna BS in the same time-frequency block. The uplink transmission is assisted by an IRS panel which consists of L reflecting elements where the i th element can introduce a phase shift θ_i to the incident signal before reflection. The direct channels between the BS and the users are assumed to be independent and identically distributed (i.i.d.) Rayleigh fading channels as the line-of-sight (LoS) path may not exist, and the direct channel between user

k and the BS is denoted as v_k . The IRS-BS and the user k -IRS channel vectors are denoted as $\mathbf{g} \in \mathbb{C}^{L \times 1}$ and \mathbf{h}_k , respectively. The IRS panel is typically set up in a position where a LoS path to the BS and to the users can be exploited. Hence, we adopt Rician fading in this paper to model the channel vectors \mathbf{g} and \mathbf{h}_k . The channel vector \mathbf{g} is given as

$$\mathbf{g} = \sqrt{\frac{PL(d_{IB})K_{IB}}{K_{IB} + 1}} \mathbf{g}^{LoS} + \sqrt{\frac{PL(d_{IB})}{K_{IB} + 1}} \mathbf{g}^{NLoS}, \quad (1)$$

where K_{IB} denotes the Rician factor of \mathbf{g} , d_{IB} is the distance between the IRS and the BS, \mathbf{g}^{LoS} and \mathbf{g}^{NLoS} are the LoS and non-LoS (NLoS) components, respectively. The LoS component is deterministic, however, the elements of \mathbf{g}^{NLoS} are i.i.d. complex normal, $\mathcal{CN}(0, 1)$, random variables. The channel vector between user k and the IRS, \mathbf{h}_k , is given as

$$\mathbf{h}_k = \sqrt{\frac{PL(d_{U_k,I})K_{UI}}{K_{UI} + 1}} \mathbf{h}_k^{LoS} + \sqrt{\frac{PL(d_{U_k,I})}{K_{UI} + 1}} \mathbf{h}_k^{NLoS}, \quad (2)$$

where K_{UI} denotes the Rician factor of \mathbf{h}_k , $d_{U_k,I}$ is the distance between user k and the IRS, \mathbf{h}_k^{LoS} and \mathbf{h}_k^{NLoS} are the LoS and NLoS components, respectively. The PL factor in the channel model represents the path loss which is modeled for all the channels as

$$PL(d) = \eta_0 \left(\frac{d}{d_0} \right)^{-\alpha}, \quad (3)$$

where η_0 is the path loss at the reference distance $d_0 = 1$ m, d represents the link distance between the transmitter and the receiver, and α is the path loss exponent.

The K users in the system transmit K data symbols simultaneously, hence, the received superimposed signal at the BS for this NOMA uplink scenario is written as

$$y = \sum_{k=1}^K (\mathbf{g}^T \mathbf{W} \mathbf{h}_k + v_k) \sqrt{p_k} s_k + n, \quad (4)$$

where s_k is the data symbol transmitted by user k , $\mathbb{E}[|s_k|^2] = 1$, p_k is the transmitted power from user k , and n is the complex Gaussian $\mathcal{CN}(0, \sigma_n^2)$ additive white Gaussian noise (AWGN) at the BS. \mathbf{W} is an $L \times L$ diagonal matrix, i.e. $\mathbf{W} = \text{diag}\{\mathbf{w}\}$, whose diagonal elements are the IRS reflection coefficients, where $\mathbf{w} = [e^{j\theta_1}, \dots, e^{j\theta_L}]^T$. The angle $\theta_i \in [0, 2\pi[$ represents the phase shift introduced by i th reflecting element.

In uplink NOMA systems, the BS performs SIC to successfully decode the K superimposed users' signals. The SIC technique requires ordering of the users according to their effective channel gains. The users with better effective channel gains are decoded first considering the other interfering signals as noise. The combined effective channel of the k th user in this system model is $\mathbf{g}^T \mathbf{W} \mathbf{h}_k + v_k$, which clearly depends on the unknown phase shifts matrix \mathbf{W} . Therefore, in this paper, we order the users according to their maximum achievable effective channel [24]. For example, for user k , we can calculate the maximum achievable effective channel gain at the BS by assuming that the IRS phases are solely optimized to maximize the channel of this user. In this case, the IRS phases should be adjusted to align all the combined IRS channels with the direct link v_k of user k , i.e., $\theta_i = \theta_{v_k} - \theta_{g_i} - \theta_{h_{ki}}$. In

this case, the maximum achievable channel gain of user k with which we order the users is calculated as $\sum_{i=1}^L |g_i| |h_{ki}| + |v_k|$. Without loss of generality, we assume that the users are arranged in a descending order as

$$\sum_{i=1}^L |g_i| |h_{1i}| + |v_1| \geq \dots \geq \sum_{i=1}^L |g_i| |h_{Ki}| + |v_K|. \quad (5)$$

Assuming successful decoding of the NOMA users at the BS using SIC, the SINR of the k th user when the BS decodes its signal can be expressed as

$$\gamma_k = \frac{p_k |\mathbf{g}^T \mathbf{W} \mathbf{h}_k + v_k|^2}{\sum_{j=k+1}^K p_j |\mathbf{g}^T \mathbf{W} \mathbf{h}_j + v_j|^2 + \sigma_n^2}, \quad (6)$$

where $\sum_{j=k+1}^K p_j |\mathbf{g}^T \mathbf{W} \mathbf{h}_j + v_j|^2 = 0$ when $k = K$, i.e., the last user in the SIC order suffers no interference. Then, the corresponding achievable data rate of the k th user is given by

$$R_k = \log_2(1 + \gamma_k), \quad \forall k. \quad (7)$$

III. TOTAL TRANSMIT POWER MINIMIZATION PROBLEM FORMULATION AND THE PROPOSED SOLUTION

In this section, we aim to minimize the sum of the transmitted powers of all the users in the multi-user IRS-assisted NOMA system assuming that each user has a minimum rate requirement that must be guaranteed to satisfy some QoS requirement at each individual user. This minimization is done by jointly optimizing the passive beamforming coefficients at the IRS, \mathbf{W} , and the power allocation at the users. Hence, the sum power minimization problem can be formulated as

$$\min_{\mathbf{p}, \mathbf{W}} \sum_{k=1}^K p_k \quad (8a)$$

$$\text{s.t.} \quad \log_2 \left(1 + \frac{p_k |\mathbf{g}^T \mathbf{W} \mathbf{h}_k + v_k|^2}{\sum_{j=k+1}^K p_j |\mathbf{g}^T \mathbf{W} \mathbf{h}_j + v_j|^2 + \sigma_n^2} \right) \geq R_k^{\min}, \quad (8b)$$

$$k = 1, 2, \dots, K,$$

$$|w_i| = 1, \quad i = 1, 2, \dots, L, \quad (8c)$$

where $w_i = e^{j\theta_i}$ is the (i, i) entry of \mathbf{W} . Solving the optimization problem in (8) is challenging because the optimization variables p_k and w_i are multiplied by each others in constraints (8b), and the constraints in (8c) are non-convex. We use the fact that we have two sets of optimization parameters, p_k 's and w_i 's, coupled together in (8), and propose an alternating optimization algorithm. The optimization problem (8) is solved alternatively in \mathbf{p} and \mathbf{W} in an iterative manner.

During each iteration n in our proposed alternating optimization algorithm, we solve the power allocation problem to get \mathbf{p}^n first for a given \mathbf{W}^{n-1} , then we optimize \mathbf{W} for a given \mathbf{p}^n to get \mathbf{W}^n , and so on. Therefore, the original problem (8) is separated into two sub-problems that are solved alternatively, as explained in the next subsections.

A. Power allocation at the users

In each iteration, for a given value of \mathbf{W} , the power allocation problem in \mathbf{p} reduces to

$$\min_{\mathbf{p}} \sum_{k=1}^K p_k \quad (9a)$$

$$\text{s.t.} \quad p_k |\mathbf{g}^T \mathbf{W} \mathbf{h}_k + v_k|^2 - (2^{R_k^{\min}} - 1) \times \left(\sum_{j=k+1}^K p_j |\mathbf{g}^T \mathbf{W} \mathbf{h}_j + v_j|^2 + \sigma_n^2 \right) \geq 0, \quad (9b)$$

$$k = 1, 2, \dots, K,$$

where the constraints in (9b) are affine inequalities in \mathbf{p} , and the objective function in (9a) is linear. Therefore, the optimization problem in (9) is a linear program in \mathbf{p} which can be easily solved using the standard simplex method using any tool such as *linprog* in MATLAB's optimization toolbox.

In the following two subsections, we present two different approaches for solving (8) in \mathbf{W} given the values of p_k 's. The two approaches are based on SDR and manifold optimization, respectively. The performance of the two approaches will be compared against each other in the results section.

B. Solve for \mathbf{W} using the SDR approach

For some given p_k values in the n th iteration, the optimization problem in (8) becomes a feasibility-check problem in \mathbf{W} , since the cost function in (8a) does not depend on the IRS reflecting coefficients \mathbf{W} . Hence, for fixed p_k values, the feasibility-check problem in \mathbf{W} is given as

$$\text{Find } \mathbf{W} \quad (10a)$$

$$\text{s.t.} \quad p_k |\mathbf{g}^T \mathbf{W} \mathbf{h}_k + v_k|^2 - (2^{R_k^{\min}} - 1) \times \left(\sum_{j=k+1}^K p_j |\mathbf{g}^T \mathbf{W} \mathbf{h}_j + v_j|^2 + \sigma_n^2 \right) \geq 0, \quad (10b)$$

$$k = 1, 2, \dots, K,$$

$$|w_i| = 1, \quad i = 1, 2, \dots, L. \quad (10c)$$

As long as the cost function in (8a) does not depend on \mathbf{W} , we propose to solve (10) in the second step of each iteration of the proposed alternating optimization algorithm to expand the feasible region of (9) in the first step of the next iteration, i.e., when optimizing \mathbf{p} given the obtained \mathbf{W} . To enhance the convergence of finding a solution to (10), the problem can be further transformed into an optimization problem with a clear objective function to find a more efficient IRS phase shifts solution, \mathbf{W} , which further reduces the total uplink transmit power of the users. The logic of this is that all the constraints are already satisfied by the optimal solution of the sum power minimization problem in (9). Therefore, optimizing the phase shifts, \mathbf{W} , to enforce the users' achievable data rates to be larger than the minimum target rates in (10) forthrightly results in the reduction of the total transmit power in (9). More specifically, we need to find a solution for \mathbf{W} that maximizes the minimum of the constraints of (10). Hence, problem (10) is converted to the following optimization problem.

$$\max_{\mathbf{W}, \alpha} \alpha \quad (11a)$$

$$\text{s.t. } p_k \left| \mathbf{g}^T \mathbf{W} \mathbf{h}_k + v_k \right|^2 - (2^{R_k^{\min}} - 1) \times \left(\sum_{j=k+1}^K p_j \left| \mathbf{g}^T \mathbf{W} \mathbf{h}_j + v_j \right|^2 + \sigma_n^2 \right) - \alpha \geq 0, \quad (11b)$$

$$k = 1, 2, \dots, K,$$

$$|w_i| = 1, \quad i = 1, 2, \dots, L, \quad (11c)$$

$$\alpha \geq 0 \quad (11d)$$

Problem (11) is non-convex because of the non-convex unit modulus constraints in (11c). However, the constraints in (11b) and (11c) can be converted into quadratic forms, then the SDR technique can be applied to find an approximate solution to (11).

The squared magnitude of the effective channel of user k can be written as

$$\left| \mathbf{g}^T \mathbf{W} \mathbf{h}_k + v_k \right|^2 = \left| \mathbf{g}^T \mathbf{H}_k \mathbf{w} + v_k \right|^2, \quad (12)$$

where $\mathbf{H}_k = \text{diag}(\mathbf{h}_k)$ and $\mathbf{w} \in \mathbb{C}^{L \times 1}$ is a column vector that contains the diagonal elements of \mathbf{W} . Then, we can expand the squared magnitude of the effective channel of the k th user as

$$\left| \mathbf{g}^T \mathbf{H}_k \mathbf{w} + v_k \right|^2 = (\mathbf{w}^H \mathbf{H}_k^H \mathbf{g}^* + v_k^*) (\mathbf{g}^T \mathbf{H}_k \mathbf{w} + v_k) \quad (13)$$

$$= (\mathbf{w}^H \mathbf{z}_k + v_k^*) (\mathbf{z}_k^H \mathbf{w} + v_k), \quad (14)$$

where $\mathbf{z}_k = \mathbf{H}_k^H \mathbf{g}^* \in \mathbb{C}^{L \times 1}$. Therefore, the squared effective channel gain of user k can be written as a quadratic term in \mathbf{w} as

$$\left| \mathbf{g}^T \mathbf{H}_k \mathbf{w} + v_k \right|^2 = \mathbf{w}^H \mathbf{z}_k \mathbf{z}_k^H \mathbf{w} + \mathbf{w}^H \mathbf{z}_k v_k + \mathbf{z}_k^H \mathbf{w} v_k^* + |v_k|^2. \quad (15)$$

Equation (15) can be expressed as $\bar{\mathbf{w}}^H \mathbf{B}_k \bar{\mathbf{w}} + |v_k|^2$, where

$$\bar{\mathbf{w}} = \begin{bmatrix} \mathbf{w} \\ 1 \end{bmatrix} \text{ and } \mathbf{B}_k = \begin{bmatrix} \mathbf{z}_k \mathbf{z}_k^H & \mathbf{z}_k v_k \\ \mathbf{z}_k^H v_k^* & 0 \end{bmatrix}. \quad (16)$$

By using the identity $\bar{\mathbf{w}}^H \mathbf{B}_k \bar{\mathbf{w}} = \text{trace}(\bar{\mathbf{w}}^H \mathbf{B}_k \bar{\mathbf{w}}) = \text{trace}(\mathbf{B}_k \bar{\mathbf{w}} \bar{\mathbf{w}}^H)$, and letting $\widehat{\mathbf{W}} = \bar{\mathbf{w}} \bar{\mathbf{w}}^H \in \mathbb{C}^{(L+1) \times (L+1)}$, we can convert the problem into a semi-definite program (SDP). The matrix $\widehat{\mathbf{W}}$ is the outer product of the vector $\bar{\mathbf{w}}$ with itself, hence $\widehat{\mathbf{W}}$ is a symmetric positive semi-definite matrix whose rank is 1. Consequently, problem (11) can be written as

$$\max_{\widehat{\mathbf{W}}, \alpha} \alpha \quad (17a)$$

$$\text{s.t. } p_k \left(\text{trace}\{\mathbf{B}_k \widehat{\mathbf{W}}\} + |v_k|^2 \right) - (2^{R_k^{\min}} - 1) \times \left(\sum_{j=k+1}^K p_j \left(\text{trace}\{\mathbf{B}_j \widehat{\mathbf{W}}\} + |v_j|^2 \right) + \sigma_n^2 \right) - \alpha \geq 0, \quad (17b)$$

$$k = 1, 2, \dots, K,$$

$$\widehat{\mathbf{W}}(i, i) = 1, \quad i = 1, 2, \dots, L, \quad (17c)$$

$$\widehat{\mathbf{W}} \succeq \mathbf{0}, \quad (17d)$$

$$\text{rank}(\widehat{\mathbf{W}}) = 1. \quad (17e)$$

Obviously, problem (17) is an SDP, however, still non-convex because of the non-convex rank one constraint in (17e). By dropping (17e), the SDP becomes convex and can be solved using readily made packages such as CVX. Neglecting the rank one constraint is the SDR of the SDP in (17). Assuming that the optimal solution obtained from solving the SDR of (17) is $\widehat{\mathbf{W}}^*$, then we need to convert $\widehat{\mathbf{W}}^*$ to a feasible solution of the original problem (11). The rank of the obtained solution, $\widehat{\mathbf{W}}^*$, of the SDR is generally greater than 1, thus we will always need to reduce our solution to a rank one matrix. An effective way to find a good rank one approximation is to select the eigenvector of $\widehat{\mathbf{W}}^*$ that corresponds to its maximum eigenvalue [31]. Assuming that the maximum eigenvalue of $\widehat{\mathbf{W}}^*$ is λ_1 and the corresponding eigenvector is \mathbf{q}_1 , then $\widehat{\mathbf{w}} = \sqrt{\lambda_1} \mathbf{q}_1$ can be considered a solution to our original problem (11). However, this solution maybe still infeasible and does not satisfy the unit modulus constraints for w_i 's. To map the solution to a nearby feasible solution, the elements of $\widehat{\mathbf{w}}$ are normalized to $\tilde{w}_i = \frac{\widehat{w}_i}{|\widehat{w}_i|}, \forall i \in \{1, \dots, L\}$.

C. Solve for \mathbf{W} using the manifold optimization approach

In this subsection, we introduce a more efficient solution for optimizing the passive beamforming vector in (10), which is the manifold optimization solution. When formulating this problem, we cannot introduce the slack variable α to the constraints, as in (11), to maximize the minimum of the constraints because the variable α does not adhere to the unit-modulus constraints as the other optimization variables, w_i . The unit-modulus constraints on the optimization variables make the feasible set of the problem have a special structure as will be discussed. Therefore, the problem of maximizing the minimum of the constraints shall be written as

$$\max_{\mathbf{W}} \min\{C_1(\mathbf{W}), C_2(\mathbf{W}), \dots, C_K(\mathbf{W})\} \quad (18a)$$

$$\text{s.t. } C_k = p_k \left| \mathbf{g}^T \mathbf{W} \mathbf{h}_k + v_k \right|^2 - (2^{R_k^{\min}} - 1) \times \left(\sum_{j=k+1}^K p_j \left| \mathbf{g}^T \mathbf{W} \mathbf{h}_j + v_j \right|^2 + \sigma_n^2 \right) \geq 0, \quad (18b)$$

$$k = 1, 2, \dots, K,$$

$$|w_i| = 1, \quad i = 1, 2, \dots, L. \quad (18c)$$

The min function in (18) is not smooth. Hence, we use a smooth and differentiable approximation as

$$\min_k |C_k| = \left(\sum_{k=1}^K C_k^{-\gamma} \right)^{-1/\gamma}, \text{ as } \gamma \rightarrow +\infty, \quad (19)$$

and $|C_k| = C_k$ because we know that all the constraints are non negative, i.e., $C_k \geq 0$. Therefore, the manifold optimization problem can be written as

$$\max_{\mathbf{W}} \left(\sum_{k=1}^K C_k^{-\gamma} \right)^{-1/\gamma} \quad (20a)$$

$$\text{s.t. } C_k \geq 0, \quad k = 1, 2, \dots, K, \quad (20b)$$

$$|w_i| = 1, \quad i = 1, 2, \dots, L. \quad (20c)$$

The unit-modulus constraints in (20c) restrict the optimization vector, \mathbf{w} , to be located on the surface of a smooth Riemannian manifold contained in \mathbb{C}^L . Precisely, all the optimization variables, w_i , lie on a continuous surface called the complex circle manifold, which is defined as

$$\mathcal{S} = \{w_i \in \mathbb{C} : |w_i| = 1\}. \quad (21)$$

The circle, \mathcal{S} , forms a smooth sub-manifold of \mathbb{C} which is a Riemannian manifold. Due to having L optimization variables in (20), the feasible set of the optimization problem is the Cartesian product of L complex circles which is given as

$$\mathcal{S}_1 \times \mathcal{S}_2 \times \dots \times \mathcal{S}_L. \quad (22)$$

The Cartesian product of smooth Riemannian manifolds forms a smooth Riemannian sub-manifold of \mathbb{C}^L . Hence, the feasible set of (20) is an L -dimensional complex circle manifold which is formally defined as

$$\mathcal{S}^L \triangleq \mathcal{S}_1 \times \dots \times \mathcal{S}_L = \{\mathbf{w} = [w_1, \dots, w_L] \in \mathbb{C}^L : |w_1| = \dots = |w_L| = 1\}. \quad (23)$$

The optimization problem in (20) has extra constraints in (20b) other than the unit-modulus constraints. In the following, we explain how we deal with the constraints given in (20b), to solve (20). We propose to handle these additional constraints by using a standard approach called the exact penalty method. To account for the constraints in (20b), the exact penalty method adds a weighted penalty term for each constraint to the the objective function being optimized. When one of the constraints is violated, the modified objective function is largely penalized by moving far away from the optimum point. By using the exact penalty method, (20) is reduced to an unconstrained optimization problem, but generally having a non-smooth objective function. Therefore, in the Riemannian case, the exact penalty method transforms (20) to an unconstrained optimization problem over the L -dimensional complex circle manifold as follows

$$\max_{\mathbf{w} \in \mathcal{M}} \left(\sum_{k=1}^K C_k(\mathbf{w})^{-\gamma} \right)^{-1/\gamma} + \rho \left(\sum_{k=1}^K \max\{0, -C_k(\mathbf{w})\} \right), \quad (24)$$

where $\rho > 0$ is a penalty weight and \mathcal{M} is the L -dimensional complex circle manifold over which the problem is optimized. Note that the constant modulus constraints in (20c) are satisfied by restricting the feasible set to the manifold \mathcal{M} . In the exact penalty method, only a finite penalty weight, ρ , is needed to exactly satisfy the constraints, hence the method's name, [32]. The penalized objective function in (24) is not smooth due to the existence of the \max functions that replace the constraints with the corresponding penalties. Therefore, we can use a smoothing technique to smooth and solve (24). By using the linear-quadratic loss approach [33], the \max function in (24) can be approximated, using a smoothing parameter $u > 0$, as $\max\{0, x\} \approx \mathcal{P}(x, u)$, where $\mathcal{P}(x, u)$ is given by

$$\mathcal{P}(x, u) = \begin{cases} 0 & x \leq 0 \\ \frac{x^2}{2u} & 0 \leq x \leq u \\ x - \frac{u}{2} & x \geq u, \end{cases} \quad (25)$$

Hence, a smooth unconstrained version of our manifold optimization problem can be written as

$$\max_{\mathbf{w} \in \mathcal{M}} Q(\mathbf{w}) = \left(\sum_{k=1}^K C_k(\mathbf{w})^{-\gamma} \right)^{-1/\gamma} + \rho \left(\sum_{k=1}^K \mathcal{P}(-C_k(\mathbf{w}), u) \right), \quad (26)$$

Thus, the problem in (20) is converted to a smooth unconstrained manifold optimization problem whose feasible points lie on the surface of the complex circle manifold, \mathcal{S}^L . In that case, we can utilize gradient-based manifold optimization techniques to solve (26).

Similar to the case of Euclidean spaces, there are two main steps for a gradient-descent based algorithm on Riemannian manifolds. Firstly, a descent direction should be found, then a step size is computed along this direction. Afterwards, the solution is updated iteratively until convergence by repeating the two steps in each iteration. However, calculating a descent direction should be adjusted to take into account the geometric nature of the manifold, which is discussed in the following. The tangent space, $T_{\mathbf{w}}\mathcal{M}$, at a point, \mathbf{w} , on a differentiable manifold, \mathcal{M} , is defined as the real vector space that intuitively contains the possible directions in which one can tangentially pass through \mathbf{w} . The tangent space at \mathbf{w} is given by

$$T_{\mathbf{w}}\mathcal{M} = \{\mathbf{v} \in \mathbb{C}^L : \Re(\mathbf{v} \odot \mathbf{w}^*) = \mathbf{0}_L\}, \quad (27)$$

where $\Re(\cdot)$ denotes the element-wise real-part of the complex vector, and \odot is the Hadamard element-wise multiplication. In the context of manifold optimization, the gradient of a function is called the *Riemannian gradient* which is defined as the direction of the steepest increase of the objective function at a certain point \mathbf{w} , and this direction must lie in the tangent space at the point \mathbf{w} . The Riemannian gradient at a point on the manifold is calculated by first calculating the Euclidean gradient at that point then projecting it onto the tangent space at the point using a projection operator. The orthogonal projection operator of a vector \mathbf{v} onto the tangent space, $T_{\mathbf{w}}\mathcal{M}$, at point \mathbf{w} on the L -dimensional complex circle manifold is given by [32]

$$P_{T_{\mathbf{w}}\mathcal{M}}(\mathbf{v}) = \mathbf{v} - \Re(\mathbf{v} \odot \mathbf{w}^*) \odot \mathbf{w}. \quad (28)$$

Hence, the Riemannian gradient of our smooth objective function Q in (26) on the manifold can be given as

$$\begin{aligned} \nabla_{\mathcal{M}}Q(\mathbf{w}) &= P_{T_{\mathbf{w}}\mathcal{M}}(\nabla Q(\mathbf{w})) \\ &= \nabla Q(\mathbf{w}) - \Re(\nabla Q(\mathbf{w}) \odot \mathbf{w}^*) \odot \mathbf{w}, \end{aligned} \quad (29)$$

where $\nabla Q(\mathbf{w})$ is the Euclidean gradient at the point \mathbf{w} . In the following, we derive the the Euclidean gradient of Q , which is required to obtain the Riemannian gradient. The Euclidean gradient is given by

$$\nabla Q(\mathbf{w}) = \left[\frac{\partial Q}{\partial w_1} \quad \frac{\partial Q}{\partial w_2} \quad \dots \quad \frac{\partial Q}{\partial w_L} \right]^T, \quad (30)$$

where $\partial Q / \partial w_i = \partial Q / \partial \Re(w_i) + j \partial Q / \partial \Im(w_i)$, and $\Im(\cdot)$ denotes the imaginary part of the complex number. Every partial derivative w.r.t. w_i is calculated as

$$\frac{\partial Q}{\partial w_i} = \frac{\partial f}{\partial w_i} + \rho \sum_{k=1}^K \frac{\partial}{\partial w_i} \mathcal{P}(-C_k(\mathbf{w}), u), \quad (31)$$

where f is the first term of the objective function Q in (26), and $\frac{\partial f}{\partial w_i}$ is computed as

$$\begin{aligned} \frac{\partial f}{\partial w_i} &= \frac{\partial f}{\partial \Re(w_i)} + j \frac{\partial f}{\partial \Im(w_i)} \\ &= \left(\sum_{k=1}^K C_k(\mathbf{w})^{-\gamma} \right)^{-1/\gamma-1} \sum_{k=1}^K C_k(\mathbf{w})^{-\gamma-1} C'_{ki}(\mathbf{w}), \end{aligned} \quad (32)$$

where $C'_{ki}(\mathbf{w})$ is calculated as

$$\begin{aligned} C'_{ki}(\mathbf{w}) &= \frac{\partial C_k(\mathbf{w})}{\partial \Re(w_i)} + j \frac{\partial C_k(\mathbf{w})}{\partial \Im(w_i)} \\ &= p_k \left(2\Re(\mathbf{d}_k^T \mathbf{w})(a_{ki} - j b_{ki}) + 2\Im(\mathbf{d}_k^T \mathbf{w})(b_{ki} + j a_{ki}) \right) \\ &\quad - (2^{R_k^{min}} - 1) \left\{ \sum_{l=k+1}^K p_l \left(2\Re(\mathbf{d}_k^T \mathbf{w})(a_{li} - j b_{li}) \right. \right. \\ &\quad \left. \left. + 2\Im(\mathbf{d}_k^T \mathbf{w})(b_{li} + j a_{li}) \right) \right\}, \end{aligned} \quad (33)$$

where $a_{ki} = \Re(h_{ki} g_i)$, $b_{ki} = \Im(h_{ki} g_i)$ and the vector $\mathbf{d}_k = \mathbf{h}_k \odot \mathbf{g}$ is the Hadamard product of the two vectors \mathbf{h}_k and \mathbf{g} . The partial derivative, $\frac{\partial \mathcal{P}(-C_k(\mathbf{w}), u)}{\partial w_i}$, is calculated as

$$\frac{\partial \mathcal{P}(-C_k(\mathbf{w}), u)}{\partial w_i} = \begin{cases} 0 & -C_k(\mathbf{w}, u) \leq 0 \\ \frac{C_k(\mathbf{w})}{u} C'_{ki}(\mathbf{w}) & 0 \leq -C_k(\mathbf{w}, u) \leq u \\ -C'_{ki}(\mathbf{w}) & -C_k(\mathbf{w}, u) \geq u, \end{cases} \quad (34)$$

where $C'_{ki}(\mathbf{w})$ is calculated in (33). Then, by substituting (32) and (34) in (31), we obtain the Euclidean gradient which is required to calculate the Riemannian gradient in (29) for our algorithm. **Algorithm 1** illustrates the steps of solving the unconstrained manifold optimization problem in (26) by updating the penalty coefficient ρ and the smoothing parameter u in an iterative manner.

The feasibility of (20) is now ensured by restricting the feasible set of the optimization problem to the complex circle manifold to satisfy the unit modulus constraints in (20c). The other constraints in (20b) are satisfied by penalizing the original cost function as in (24) using the exact penalty method.

Next, we investigate the behavior of **Algorithm 1** and explain how the parameters ρ and u are updated in each iteration. First, we need to mention that the optimum points of the penalized unconstrained problem in (26) are the same as the optimum points of the original problem in (20) when the penalty coefficient ρ is higher than a certain threshold [32]. This threshold is usually unknown; hence, we adopt a common iterative approach provided in [34] to address this problem. This approach does not start with a large ρ because this may slow down the convergence of **Algorithm 1**. Therefore, **Algorithm 1** starts with a relatively low initial value of ρ_0 , then this value is increased in each iteration, by multiplying it by the constant $\theta_\rho > 1$, if the constraints in (20b) are violated as shown in lines 8 and 9 in **Algorithm 1**. The parameter τ is a tolerance factor which is a low positive number so that if $-C_k(\mathbf{w}_{l+1})$ surpasses τ , the point \mathbf{w}_{l+1} is considered out of the feasible region and ρ must be increased.

Algorithm 1: Exact penalty method via smoothing

```

1 Input: Starting point  $\mathbf{w}_0$ , starting penalty coefficient
    $\rho_0$ , starting smoothing accuracy  $u_0$ , minimum
   smoothing accuracy  $u_{\min}$ , constants  $\theta_u \in (0, 1)$ ,
    $\theta_\rho > 1$ ,  $\tau \geq 0$ , minimum step length  $d_{\min}$ .
2 for  $l = 0, 1, 2, \dots$  do
3   To obtain  $\mathbf{w}_{l+1}$ , choose any sub-solver to
   approximately solve
       
$$\min_{\mathbf{w} \in \mathcal{M}} Q(\mathbf{w}, \rho_l, u_l)$$

   with warm-start at  $\mathbf{w}_l$  and stopping criterion
       
$$\|\text{grad } Q(\mathbf{w}, \rho_l, u_l)\| \leq \delta.$$

4   if
    $(\text{dist}(\mathbf{w}_l, \mathbf{w}_{l+1}) < d_{\min} \text{ or } u_l \leq u_{\min})$  and  $C_k(\mathbf{w}_{l+1}) < \tau$ 
   then
5     | Return  $\mathbf{w}_{l+1}$ ;
6   end
7    $u_{l+1} = \max\{u_{\min}, \theta_u u_l\}$ ;
8   if  $(l = 0 \text{ or } -C_k(\mathbf{w}_{l+1}) \geq \tau)$  then
9     |  $\rho_{l+1} = \theta_\rho \rho_l$ 
10  else
11  |  $\rho_{l+1} = \rho_l$ ;
12  end
13 end

```

The approximation function in (34) is more accurate when the smoothing parameter u_l is decreased. However, if u_l is too small, numerical difficulties may arise when using the approximation function in (34). Consequently, **Algorithm 1** starts with u_0 , then keeps decreasing u_l , by multiplying it with the constant fraction θ_u , in each iteration, as in line 7, until it reaches a minimum value u_{\min} . **Algorithm 1** terminates when the Euclidean distance between \mathbf{w}_{l+1} and \mathbf{w}_l is smaller than d_{\min} . To solve the unconstrained optimization problem in line 3 in each iteration, we use the trust region manifold optimization solver [32], that exists in *Manopt* MATLAB toolbox [35], by setting a stopping criterion on the gradient norm.

D. Convergence of the alternating optimization discussion

In both alternating optimization solutions discussed in the previous subsections, i.e. SDR and manifold schemes, we solve the original problem in (8) by solving the power allocation problem in (9) and the passive beamforming problem at the IRS in (11) using SDR, or in (18) using manifold optimization, alternately in an iterative manner. In each iteration, we get a solution that is used as the initial point for the next iteration. Specifically, the alternating optimization algorithm starts with solving problem (9) for a given beamforming vector \mathbf{w} rather than solving (11) or (18) for a given \mathbf{p} . This is intentionally designed because (9) is always feasible in \mathbf{p} for any beamforming vector \mathbf{w} , however, (11) or (18) may not always be feasible for any arbitrary \mathbf{p} . Intuitively, when the obtained solution from (11) or (18) achieves a higher user uplink rate than the target minimum rate constraint for user k ,

then the transmit power of user k can be suitably decreased while maintaining all the rate constraints. Consequently, the total transmit power in (9) can be reduced accordingly.

More precisely, we can ensure the convergence of the proposed alternating optimization solution for (8) using the following. We can deduce that the cost function of (9), which is the sum transmit powers at the users, is non-increasing over the iterations when solving (9) and (11) or (18) iteratively using our proposed alternating optimization algorithm. This proposition can be proved as follows. Assume that the objective value of (9), based on the a certain IRS coefficients vector \mathbf{w} , is denoted as $f(\mathbf{w}, \mathbf{p})$, where \mathbf{p} denotes the transmit power vector of the users. In the n th iteration in the alternating optimization scheme, if a feasible solution to (11) or (18) exists, i.e. $(\mathbf{w}^n, \mathbf{p}^n)$, then this solution is also feasible to problem (9). Then, it follows that $f(\mathbf{w}^n, \mathbf{p}^{n+1}) \stackrel{(a)}{\leq} f(\mathbf{w}^n, \mathbf{p}^n) \stackrel{(b)}{=} f(\mathbf{w}^{n-1}, \mathbf{p}^n)$; (a) follows because for a given \mathbf{w}^n , \mathbf{p}^{n+1} is the optimal solution to problem (9). Moreover, (b) follows since the objective function of (9) does not depend on \mathbf{w} and is only affected by \mathbf{p} .

IV. ENERGY EFFICIENCY MAXIMIZATION PROBLEM AND THE PROPOSED SOLUTION

In this section, EE maximization is discussed for the uplink NOMA scenario in Fig. 1. The EE of our considered system model is defined as the ratio of the achievable sum-rate of the K users in the NOMA resource block over the total sum of the consumed transmission power by the users. Our objective in this section is to maximize EE while guaranteeing the minimum QoS constraint at each user, i.e., $R_k \geq R_k^{min}$. The achievable sum rate of the NOMA scheme can be rewritten as

$$\begin{aligned} R^{sum} &= \sum_{k=1}^K \log_2 \left(1 + \frac{p_k |\mathbf{g}^T \mathbf{W} \mathbf{h}_k + v_k|^2}{\sum_{j=k+1}^K p_j |\mathbf{g}^T \mathbf{W} \mathbf{h}_j + v_j|^2 + \sigma_n^2} \right) \\ &= \log_2 \left(1 + \frac{\sum_{k=1}^K p_k |\mathbf{g}^T \mathbf{W} \mathbf{h}_k + v_k|^2}{\sigma_n^2} \right). \end{aligned} \quad (35)$$

Therefore, our considered EE maximization is formulated as

$$\max_{\mathbf{p}, \mathbf{w}} \frac{\log_2 \left(1 + \frac{\sum_{k=1}^K p_k |\mathbf{g}^T \mathbf{H}_k \mathbf{w} + v_k|^2}{\sigma_n^2} \right)}{\sum_{k=1}^K p_k} \quad (36a)$$

$$\text{s.t. } C_k(\mathbf{w}, \mathbf{p}) \geq 0, \quad k = 1, 2, \dots, K, \quad (36b)$$

$$|w_i| = 1, \quad i = 1, 2, \dots, L, \quad (36c)$$

where $\mathbf{H}_k = \text{diag}(\mathbf{h}_k)$ and \mathbf{w} is a column vector that contains the diagonal elements of \mathbf{W} . We propose to solve (36) using alternating optimization as in the previous section because we have two blocks of optimization parameters \mathbf{p} and \mathbf{w} . In the next subsections, we first solve the problem in \mathbf{p} given \mathbf{w} , then the problem is solved in \mathbf{w} given \mathbf{p} .

A. Optimizing the transmit power vector for a given beamforming vector

Given the beamforming vector \mathbf{w} , the optimizing (36) is a non-linear fractional program in \mathbf{p} which can be expressed as

$$\max_{\mathbf{p}} \frac{\log_2 \left(1 + \frac{\sum_{k=1}^K p_k a_k}{\sigma_n^2} \right)}{\sum_{k=1}^K p_k} \quad (37a)$$

$$\text{s.t. } C_k(\mathbf{p}; \mathbf{w}) \geq 0, \quad k = 1, 2, \dots, K, \quad (37b)$$

where $a_k = |\mathbf{g}^T \mathbf{H}_k \mathbf{w} + v_k|^2$. The feasible set of (37) is convex since all the constraints are affine in \mathbf{p} . The fractional objective function has a concave numerator w.r.t. $p_k, k \in \{1, \dots, K\}$, while the denominator is an affine mapping over the feasible set of \mathbf{p} . Therefore, this non-linear fractional program is *pseudo-concave* and has an optimal solution that can be efficiently obtained using the iterative Dinkelbach's algorithm [36]. The specific procedure of this algorithm is summarized in **Algorithm 2**. During each iteration, the proposed algorithm needs to solve the following problem

$$\max_{\mathbf{p}} \log_2 \left(1 + \frac{\sum_{k=1}^K p_k a_k}{\sigma_n^2} \right) - \beta \left(\sum_{k=1}^K p_k \right) \quad (38)$$

$$\text{s.t. } (37b)$$

where β is a known constant. Obviously, (38) is concave and its feasible set is convex, hence it can be solved using standard optimization algorithms like the interior point method. Nonetheless, (38) has a specific structure that can be exploited to develop a low complexity solutions. The standard approaches are computationally intensive especially that solving (38) is repeated in each iteration of **Algorithm 2**.

Algorithm 2: EE max. for \mathbf{p}

- 1 **Initialize parameters:** $\epsilon > 0, \beta = 0, F > \epsilon$.
 - 2 **while** $F > \epsilon$ **do**
 - 3 $\mathbf{p}^* =$
 $\arg \max \log_2 \left(1 + \frac{\sum_{k=1}^K p_k a_k}{\sigma_n^2} \right) - \beta \left(\sum_{k=1}^K p_k \right);$
 s.t. (36b);
 - 4 $F = \log_2 \left(1 + \frac{\sum_{k=1}^K p_k^* a_k}{\sigma_n^2} \right) - \beta \left(\sum_{k=1}^K p_k^* \right);$
 - 5 $\beta = \frac{\log_2 \left(1 + \frac{\sum_{k=1}^K p_k^* a_k}{\sigma_n^2} \right)}{\sum_{k=1}^K p_k^*};$
 - 6 **end**
-

In the following, we propose a low-complexity optimal solution for (38) to reduce the computational load since **Algorithm 2** requires solving (38) many times. Let $F = \log_2 \left(1 + \frac{\sum_{k=1}^K p_k a_k}{\sigma_n^2} \right) - \beta \left(\sum_{k=1}^K p_k \right)$, then the partial derivative of F w.r.t. p_k is calculated as

$$\frac{\partial F}{\partial p_k} = \frac{a_k}{(\ln 2)(\sum_{i=1}^K p_i a_i + \sigma_n^2)} - \beta. \quad (39)$$

By setting $\partial F / \partial p_k = 0$, we get

$$p_k^* = 1 / (\beta \ln 2) - \left(\sum_{i \neq k} p_i a_i + \sigma_n^2 \right) / a_k. \quad (40)$$

We calculate p_k^* assuming all the remaining $p_i \forall i \neq k$ values are fixed, and this process is repeated until convergence. On this basis, the proposed low-complexity algorithm goes as follows: we first allocate the minimum required power for

each user; then, we update the power for the users one by one as illustrated in **Algorithm 3**; this update continues until convergence. Note that the convergence is guaranteed since F increases or remains unchanged after each update, and F has an upper bound. Moreover, the obtained local optimum is also the global optimum since the cost function F in (38) is concave. p_k^{\min} and p_k^{\max} in **Algorithm 3** are simply calculated for each user according to its boundaries as in the constraints in (37b).

Algorithm 3: Low complexity and fast iterative solution for solving step 3 in **Algorithm 2**

```

1 Initialize: Set  $p_k = p_k^{\min}$ ,  $k = 1, 2, \dots, K$ ;
2 while 1 do
3    $\mathbf{p}_{old} = \mathbf{p}$ ;
4   for  $k = 1:K$  do
5      $p_k^* = 1/(\beta \ln 2) - (\sum_{i \neq k} p_i a_i + \sigma_n^2)/a_k$ ;
6     if  $p_k^* < p_k^{\min}$  then
7        $p_k = p_k^{\min}$ ;
8     end
9     if  $p_k^* > p_k^{\max}$  then
10       $p_k = p_k^{\max}$ ;
11     end
12     if  $p_k^{\min} < p_k^* < p_k^{\max}$  then
13        $p_k = p_k^*$ ;
14     end
15   end
16   if  $|\mathbf{p}_{old} - \mathbf{p}| < 10^{-10}$  then
17     break while loop;
18   end
19 end

```

B. Optimizing the IRS coefficients vector \mathbf{w} given \mathbf{p}

In this subsection, we discuss the step of optimizing the IRS coefficients vector \mathbf{w} given the transmit power vector \mathbf{p} for the sake of maximizing the EE of the NOMA system using the alternating maximization algorithm. Both the SDR and manifold optimization based solutions are proposed in this subsection as presented for the total transmit power minimization problem in Sec. III. Unlike the total transmit power minimization problem, in the EE maximization problem, we have a direct objective function of \mathbf{w} to be maximized when optimizing the coefficients vector \mathbf{w} for a given \mathbf{p} . When maximizing the objective function in (36a) w.r.t. \mathbf{w} , the denominator is neglected because it is considered as a constant as it is not a function of \mathbf{w} . Hence, we only focus on the numerator which is the log function. Moreover, the log function is monotonically increasing, hence we can only focus on maximizing its argument. Therefore, when considering the SDR optimization scheme using the same mathematical steps as in Sec. III-B, the NOMA EE maximization problem in \mathbf{w}

can be written as

$$\max_{\widehat{\mathbf{W}}} \sum_{k=1}^K p_k (\text{trace}\{\mathbf{B}_k \widehat{\mathbf{W}}\} + |v_k|^2) \quad (41a)$$

$$\text{s.t.} \quad p_k (\text{trace}\{\mathbf{B}_k \widehat{\mathbf{W}}\} + |v_k|^2) - (2R_k^{\min} - 1) \times \left[\sum_{j=k+1}^K p_j (\text{trace}\{\mathbf{B}_j \widehat{\mathbf{W}}\} + |v_j|^2) + \sigma_n^2 \right] \geq 0, \quad (41b)$$

$$k = 1, 2, \dots, K,$$

$$\widehat{\mathbf{W}}(i, i) = 1, \quad i = 1, 2, \dots, L, \quad (41c)$$

$$\widehat{\mathbf{W}} \succeq \mathbf{0}, \quad (41d)$$

$$\text{rank}(\widehat{\mathbf{W}}) = 1, \quad (41e)$$

where $\widehat{\mathbf{W}} = \bar{\mathbf{w}}\bar{\mathbf{w}}^H$ and $\bar{\mathbf{w}}$ is defined in (16). Similar to the SDR problem in (17), the problem in (41) is an SDP which is non-convex due to the non-convex rank one constraint in (41e). By dropping (41e), (41) becomes clearly convex which can be directly solved using the available optimization tools such as CVX.

We can also use the manifold optimization scheme to optimize the IRS coefficients vector, \mathbf{w} , given \mathbf{p} when maximizing EE. As discussed in Sec. III-C, the unit modulus constraints on the elements of \mathbf{w} restrict the feasible region to the complex circle manifold \mathcal{M} . Hence, the EE manifold optimization problem can be written as

$$\max_{\mathbf{w} \in \mathcal{M}} \sum_{k=1}^K p_k |\mathbf{g}^T \mathbf{H}_k \mathbf{w} + v_k|^2 \quad (42a)$$

$$\text{s.t.} \quad C_k(\mathbf{w}) \geq 0, \quad k = 1, 2, \dots, K. \quad (42b)$$

Following the same procedures as in Sec. III-C, the problem in (42) is transformed to an unconstrained manifold optimization problem using the exact penalty method. Then, we shall use the same smoothing technique as discussed in Sec. III-C to smooth the unconstrained penalized optimization problem. Therefore, the smooth unconstrained NOMA EE manifold optimization problem, in \mathbf{w} given \mathbf{p} , can be written as

$$\max_{\mathbf{w} \in \mathcal{M}} \sum_{k=1}^K p_k |\mathbf{g}^T \mathbf{H}_k \mathbf{w} + v_k|^2 + \rho \left(\sum_{k=1}^K \mathcal{P}(-C_k(\mathbf{w}), u) \right), \quad (43)$$

where \mathcal{P} is the smoothing function defined in (25). Now, the unconstrained problem in (43) is smooth and differentiable which can be solved using the manifold optimization toolbox as discussed in Sec. III-C. The parameters ρ and u in (43) are updated in the same way illustrated in **Algorithm 1**.

Surprisingly, as shown in the simulation results in Sec. VI, we found that focusing on expanding the feasible set of the problem in \mathbf{p} by finding the beamforming coefficients vector \mathbf{w} , that maximizes the minimum of the constraints $C_k(\mathbf{w})$, is more suitable for the EE maximization problem than maximizing the EE objective function itself. This can be done by the alternation between solving the problem (37) in \mathbf{p} given \mathbf{w} , then solving the problem (26) in \mathbf{w} given \mathbf{p} in an iterative manner. This approach is counter-intuitive as

it optimizes the IRS beamforming vector during \mathbf{w} phase to expand the feasible set of the power allocation problem in (37) during \mathbf{p} phase, rather than maximizing the EE itself which is the target of the problem. However, the presented simulation results in Sec. VI show that this approach gives way better EE performance than focusing on maximizing the objective function discussed earlier in this section. The reason behind this behavior is that we optimize the passive beamforming vector, \mathbf{w} , to expand the feasible region over which the power allocation problem in (37) is optimized during the alternating optimization algorithm. Therefore, when maximizing the EE objective function in the power allocation phase in (37), **Algorithm 2** can search over a larger feasible set to maximize the EE of the system which may increase the value of the obtained EE in the next iteration of the alternation maximization algorithm.

V. COMPARISON WITH OPTIMIZED IRS-ASSISTED OMA

In this section, we discuss the IRS assisted uplink OMA scenario for comparison-sake. We study the average transmit power minimization and EE maximization problems for this case, as we did in the NOMA case, and provide an optimal solution for both problems.

A. IRS-assisted OMA power minimization

In this subsection, we present an optimal solution for minimizing the average transmit power of the OMA users when assisted by IRS. The sum transmit power is minimized while having minimum uplink rate constraints for the users. In the OMA scheme, each user takes a fraction of the time frame to transmit its data. Unlike the NOMA scheme, in the IRS assisted OMA, each user transmits its data separately within its allocated time fraction, α_k , while other users remain idle. This time allocation for the users, α_k , is optimized along with the transmit powers, p_k , to minimize the average transmit power of the users. This optimization problem can be expressed as

$$\min_{\alpha_k, p_k} \sum_{k=1}^K \alpha_k p_k \quad (44a)$$

$$\text{s.t. } \alpha_k \log_2 \left(1 + \frac{p_k c_k}{\sigma_n^2} \right) \geq R_k^{\min}, \quad k = 1, 2, \dots, K, \quad (44b)$$

$$\alpha_k \geq 0, \quad (44c)$$

$$\sum_{k=1}^K \alpha_k = 1, \quad (44d)$$

where $c_k = |\mathbf{g}^T \mathbf{W}_k \mathbf{h}_k + v_k|^2$. As long as the users send their data separately during their allocated time, the IRS adjusts its phase shifts, \mathbf{W}_k , independently of each user according to the corresponding channel vector, \mathbf{h}_k , as each user experiences an *interference-free* channel. The IRS phase shifts are chosen so that all the elements of the cascaded user-IRS-BS channel, $h_{ki} w_i g_i \forall i$, are aligned to have the same phase which is the phase of the direct channel v_k , i.e., $\theta_i = \theta_{v_k} - \theta_{g_i} - \theta_{h_{ki}}$. To minimize the average transmit power of the OMA users, the minimum rate constraints in (44b) shall be satisfied with

equality in order to reduce p_k as much as possible. When the constraints in (44b) are satisfied with equality, the power of each user p_k can be expressed in a closed-form as

$$p_k = \frac{\sigma_n^2}{c_k} \left(2^{R_k^{\min}/\alpha_k} - 1 \right). \quad (45)$$

By eliminating p_k from (44a), (44) can be reduced to

$$\min_{\alpha_k} \sum_{k=1}^K \frac{\sigma_n^2 \alpha_k}{c_k} \left(2^{R_k^{\min}/\alpha_k} - 1 \right) \quad (46a)$$

$$\text{s.t. } \alpha_k \geq 0, \quad (46b)$$

$$\sum_{k=1}^K \alpha_k = 1. \quad (46c)$$

The feasible set of the optimization problem in (46) is clearly convex since the constraints (46b) and (46c) are affine in α_k . Now, we need to check the convexity of the objective function in (46a). The objective function is separable in α_k 's, i.e. it can be written as a sum of separate terms in $\alpha_1, \alpha_2, \dots, \alpha_K$. Therefore, the Hessian matrix of (46a) is diagonal as $\frac{\partial^2 f_{oma}}{\partial \alpha_k \partial \alpha_j} = 0, k \neq j$, where f_{oma} is the objective function in (46a). Since the Hessian matrix is diagonal, its eigenvalues are the diagonal elements themselves, which can be calculated as

$$\frac{\partial^2 f_{oma}}{\partial \alpha_k^2} = \frac{\sigma_n^2}{c_k} \frac{((\ln 2) R_k^{\min})^2}{\alpha_k^3} 2^{(R_k^{\min}/\alpha_k)}, \quad (47)$$

where $\frac{\partial^2 f_{oma}}{\partial \alpha_k^2}$ is the second partial derivative of f_{oma} w.r.t. α_k . Clearly, the second derivatives in (47) are always positive over the feasible set of (46) since α_k 's are non-negative. Consequently, (46) is strictly convex since it has a convex feasible set as well as a convex objective function, then it can be efficiently solved using CVX or MATLAB's `fmincon` function in the optimization toolbox.

B. IRS-assisted OMA EE maximization

In this subsection, we present the EE maximization problem of the OMA system and propose an optimal solution for it. The EE maximization problem is solved under minimum uplink data rate constraints for the users. The EE maximization problem of the OMA system can be formulated as

$$\max_{\alpha_k, p_k} \frac{\sum_{k=1}^K \alpha_k \log_2 \left(1 + \frac{p_k c_k}{\sigma_n^2} \right)}{\sum_{k=1}^K \alpha_k p_k} \quad (48a)$$

$$\text{s.t. } \alpha_k \log_2 \left(1 + \frac{p_k c_k}{\sigma_n^2} \right) \geq R_k^{\min}, \quad (48b)$$

$$k = 1, 2, \dots, K, \quad (48c)$$

$$\alpha_k \geq 0, \quad (48c)$$

$$\sum_{k=1}^K \alpha_k = 1, \quad (48d)$$

where $c_k = |\mathbf{g}^T \mathbf{W}_k \mathbf{h}_k + v_k|^2$ and \mathbf{W}_k is adjusted to maximize the value of c_k as discussed in the previous subsection. Assuming that c_1 is greater than the values of c_k of other users, then we focus on allocating all the excess power to user

1, i.e., increasing p_1 , while the powers of the other users are chosen to satisfy their minimum rate constraints with equality. Therefore, the EE maximization problem reduces to

$$\max_{\alpha_k, p_1} \frac{\alpha_1 \log_2 \left(1 + \frac{p_1 c_1}{\sigma_n^2} \right) + \sum_{k=2}^K R_k^{min}}{\alpha_1 p_1 + \sum_{k=2}^K \alpha_k \left[2^{R_k^{min}/\alpha_k} - 1 \right] * \frac{\sigma_n^2}{c_k}} \quad (49a)$$

$$\text{s.t. } \alpha_1 \log_2 \left(1 + \frac{p_1 c_1}{\sigma_n^2} \right) \geq R_1^{min}, \quad (49b)$$

$$\alpha_k \geq 0, \quad (49c)$$

$$\sum_{k=1}^K \alpha_k = 1. \quad (49d)$$

Problem (49) is solved using alternating maximization over p_1 and α_k iteratively until convergence. It can be readily proved that the problem in (49) is concave w.r.t. p_1 . However, (49) is quasi-concave in α_k since the numerator is affine and the denominator is convex w.r.t. α_k as proved in the previous subsection. Therefore, the Dinkelbach algorithm discussed in Sec. IV-A can be used to solve (49) w.r.t. α_k .

VI. SIMULATION RESULTS

In this section, we provide extensive simulation results to validate the proposed optimization algorithms for IRS assisted uplink NOMA systems. The proposed solutions are compared against the IRS assisted OMA under different scenarios. For each optimization problem, we compare the performance of the SDR based solution against the manifold optimization-based solution to demonstrate the superiority of the proposed scheme. Under each scenario, we present the results in terms of the total transmit power, the EE, and the achievable uplink sum rate of the proposed solution. Comparing these three system performance measures of the total transmit power minimization problem against those of the EE maximization problem reveals very useful insights which relate the two problems. The two problems are solved and compared against each other under two scenarios; the first is when low minimum target uplink rates are required for the users, and the second is when high minimum rate constraints are required for the users. These comparisons are made for 2 and 3 users per NOMA cluster.

The following are the simulation parameters used [11], [25]. The distance between the BS and the IRS is assumed $d_{IB} = 75$ m. The distances between the users and the IRS are $\{10, 20\}$ m and $\{10, 20, 40\}$ m for the cases of 2 and 3 users per NOMA cluster, respectively. The distances between the users and the BS are $\{30, 50\}$ m and $\{30, 50, 200\}$ m for the cases of 2 and 3 users per NOMA cluster, respectively. The path loss at the reference distance in (3) is $\eta_0 = 10^{-3}$, and the path loss exponents for the direct links (users to BS), IRS to users links and BS to IRS link are assumed in this simulation setup as $\alpha_{BU} = 5.5$, $\alpha_{IU} = 2.2$ and $\alpha_{BI} = 2.2$, respectively. The noise power σ_n^2 is set to be -114 dBm, and the Rician factors in (1) and (2) are set to be $K_{IB} = K_{UI} = 2.2$.

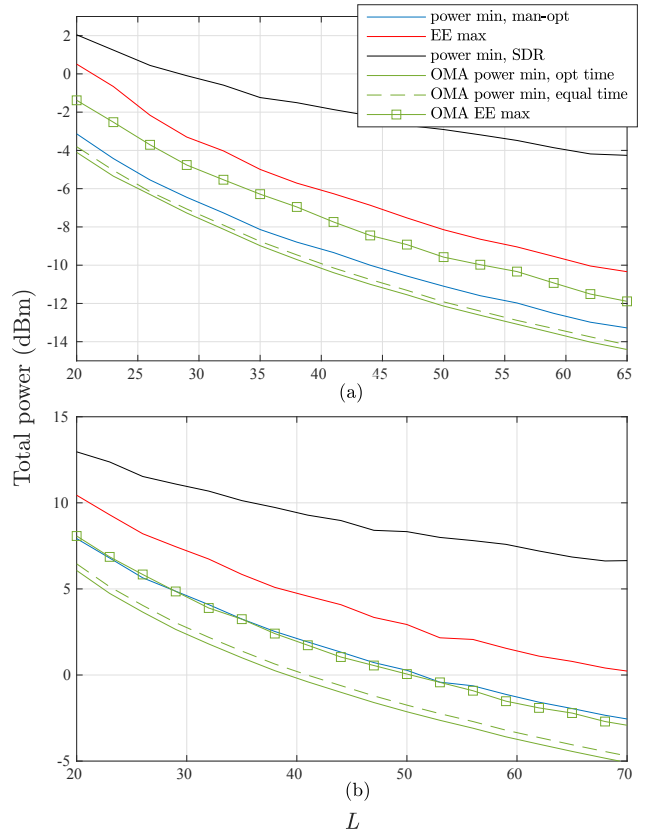


Figure 2: Sum power vs. number of reflectors L for low rate (a) 2-users cluster, (b) 3-user cluster

A. Comparing NOMA vs. OMA assuming low minimum rate constraints at the users

In Fig. 2, we present the total transmission power of the users versus the number of reflecting elements at the IRS for the different schemes, assuming 2 and 3 users in the NOMA cluster in sub-figures (a) and (b), respectively. Low minimum rate QoS constraints at the users are assumed in Fig. 2 where the minimum target achievable rates at the users are set at 0.2 bits/sec/Hz. We compare the performance of the proposed manifold optimization scheme against the common SDR optimization scheme and the IRS-assisted OMA scheme. The figure shows that our proposed manifold optimization scheme is far superior to the common SDR scheme that is widely used in the literature of IRS-assisted wireless networks. The total transmit power of the users when using the proposed manifold optimization approach is far less than its value when using the SDR based optimization approach, and the gap between the two schemes increases as the number of reflectors, L , increases. Fig. 2 also shows that the IRS assisted OMA scheme outperforms the NOMA scheme for the case of low minimum target rate requirements at the users. This shows that the IRS assisted OMA is preferred over the IRS assisted NOMA when low minimum rate constraints are required at the users. The graph also compares the total transmit power of the users resulting from solving the sum power minimization problem against the total power resulting from solving the EE maximization problem for both NOMA and OMA cases.

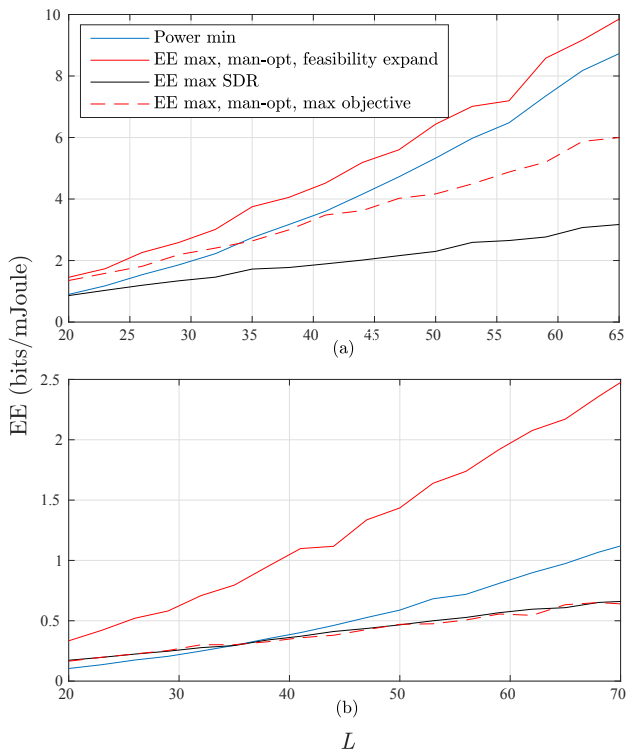


Figure 3: EE vs. number of reflectors L for low rate (a) 2-users cluster, (b) 3-user cluster

Clearly, and as expected, the graph shows that the sum power curve of the EE maximization problem is higher than the total power resulting from the power minimization problem. The rationale behind this is that the EE objective function, in (37a) for the NOMA case or in (48a) for the OMA case, is pseudo concave w.r.t. the transmit power vector \mathbf{p} . Hence, when the target uplink rate constraints are low, the minimum transmit powers of the users must be low too, which makes the system's EE far from the maximum EE point of the pseudo concave objective function. Therefore, in the case of low rate constraints, moving towards the maximum EE point requires increasing the transmit powers of the users above the minimum. That is why the power consumption in the case of NOMA/OMA EE maximization is higher than the power consumption in the case of total transmit power minimization.

Fig. 3 shows the performance of the proposed EE maximization solutions using the alternation maximization scheme discussed in Sec. IV for the cases of 2 and 3 users per NOMA cluster in sub-figures (a) and (b), respectively. The IRS-assisted NOMA EE maximization problem is solved by optimizing \mathbf{p} given fixed \mathbf{w} using **Algorithm 2**, then optimizing \mathbf{w} given fixed \mathbf{p} alternately using the alternation maximization algorithm. When solving for \mathbf{w} given \mathbf{p} , we compare the proposed solution using the SDR scheme against the solution using manifold optimization scheme discussed in Sec. IV-B. Fig. 3 shows a wide performance gain of the obtained EE using manifold optimization over the obtained EE using SDR. The SDR method in the EE maximization problem fails to provide good results compared to the manifold optimization solution. From Fig. 3, and as expected, we can

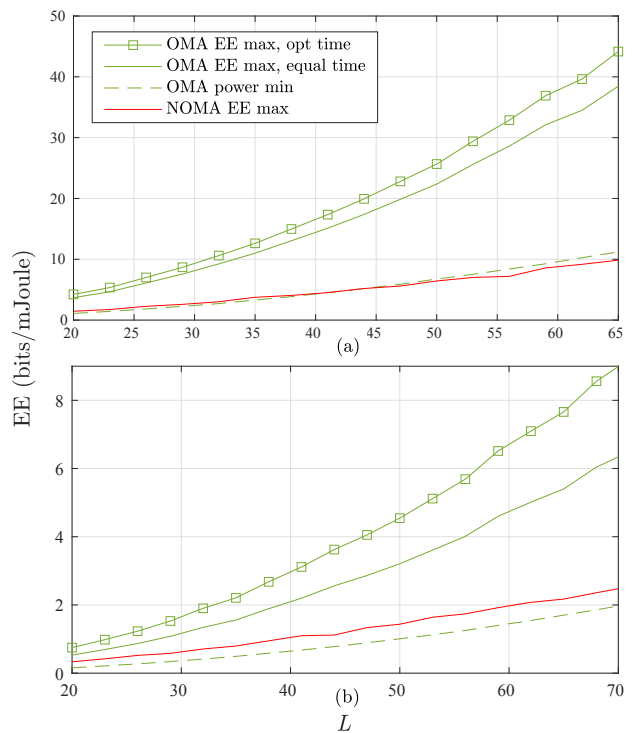


Figure 4: Comparison between OMA and NOMA EE for low rate (a) 2-users cluster, (b) 3-user cluster

also see that the EE resulting from minimizing the total power in (8) is lower than that of the problem directly maximizing the EE in (36). In this case, the users are permitted to increase their transmit powers and hence increase their uplink data rates accordingly above the minimum target rates for the sake of increasing EE.

Fig. 4 compares the EE of the IRS assisted OMA scheme against the EE of the NOMA counterpart for the case of low minimum uplink rate constraints at the users. The figure shows the comparison between the OMA and the NOMA schemes with 2 and 3 users per cluster in sub-figures (a) and (b), respectively. The graph shows that the resultant EE of the OMA scheme largely beats the EE of the NOMA scheme in the case of low uplink QoS requirements at the users. Fig. 4 also shows that optimizing the time allocations of the IRS assisted OMA scheme, by solving problem (48) in Sec. V-B, results in higher EE than the regular OMA scheme with equal time fractions among the users. The figure also compares the resultant EE of the OMA scheme when the objective is minimizing the total transmit power against the EE resulted from maximizing the EE of the system. Intuitively, the resultant EE of maximizing the OMA system's EE is higher than the resultant EE of minimizing the OMA total transmit power. This is because the OMA EE objective function in (48a) is pseudo concave w.r.t. the transmit power vector \mathbf{p} . When the target uplink rate constraints are low, the user transmit at low power levels in the case of total transmit power minimization, which makes them far behind the maximum EE point. Therefore, in the case of OMA EE maximization, the users increase their transmit powers moving towards the

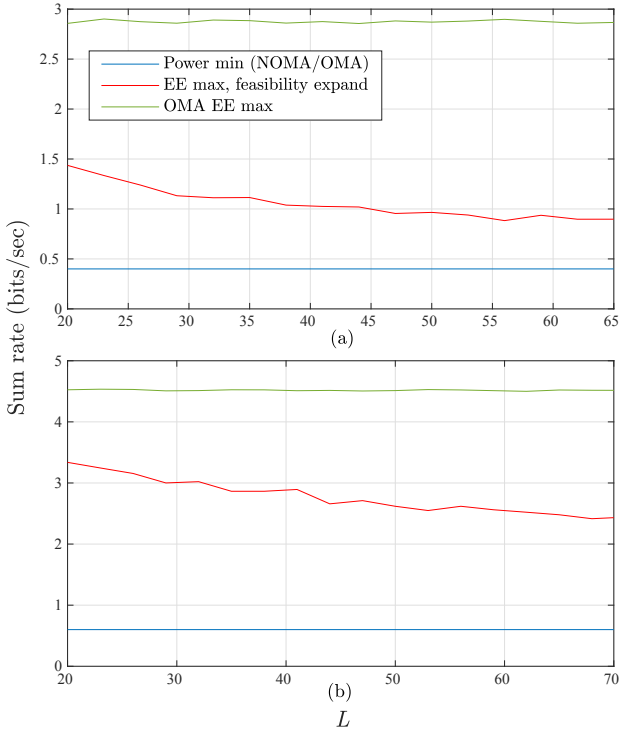


Figure 5: Sum rate vs. number of reflectors L for low rate (a) 2-users cluster, (b) 3-user cluster

maximum EE point of the OMA system. However, in the case of minimizing the total transmit power, we only focus on minimizing the transmit power as much as possible by satisfying the minimum target uplink rates with equality while neglecting the EE aspect.

In Fig. 5, we plot the achievable sum rate of the users in the system that corresponds to solving the two optimization problems we discuss in this paper. Clearly, when solving the total transmit power minimization problem in NOMA/OMA system, each user exactly achieves the target minimum required uplink rate with equality. This is intuitive since the main target is to minimize the transmit powers of the users as much as possible when solving the total transmit power minimization problem. However, when solving the EE maximization problem in NOMA/OMA system, the users are allowed to transmit at higher power levels achieving higher uplink data rates to maximize the overall EE of the system. The illustration of this behaviour is that, as discussed in Fig. 2, the NOMA and OMA EE cost functions in (37a) and (48a), respectively, are pseudo concave in the transmit power vector \mathbf{p} . Therefore, when the target uplink rate constraints are low, the users increase their transmit power moving towards the maximum EE point of the system. As a result, the achievable uplink data rates of the users increase accordingly beyond the target minimum rates when solving the EE maximization problem for both NOMA and OMA systems.

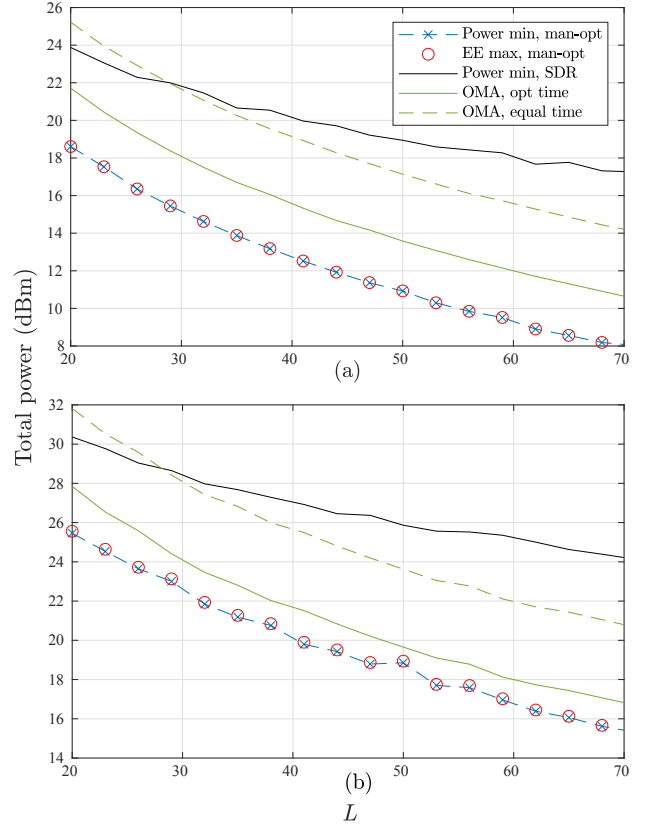


Figure 6: Sum power vs. number of reflectors L for high rate (a) 2-users cluster, (b) 3-users cluster

B. Comparing NOMA vs. OMA assuming high minimum rate constraints at the users

In the next figures, we show the performance of the proposed solutions to both the total transmit power minimization problem and the EE maximization problem when the minimum target uplink rates are high. We assume that the target minimum transmission rate for each user is 4 and 2.5 bits/sec/Hz for the cases of 2 and 3 users per NOMA cluster, respectively. We will show how the two optimization problems are related when the target transmission rates of the users are high.

Fig. 6 shows the total uplink transmit power of the users versus the number of reflecting elements for the different schemes assuming 2 and 3 users in the NOMA cluster in sub-figures (a) and (b), respectively. We compare the performance of the proposed manifold scheme against the SDR one, and the IRS-assisted OMA scheme. Similar to the low rate constraints case, Fig. 6 shows that our proposed approach is far superior to the SDR one in the case of high rate constraints too. Unlike the case of low rate constraints, Fig. 6 shows that the IRS assisted NOMA scheme outperforms the optimized OMA scheme in the case of high minimum rate requirements at the users. This shows that the IRS assisted NOMA is preferred over the IRS assisted OMA when high minimum target rate constraints are required. Fig. 6 also compares the total transmit power of the users resulting from solving the sum power minimization problem against the total power resulting from solving the EE maximization problem for both NOMA and OMA cases.

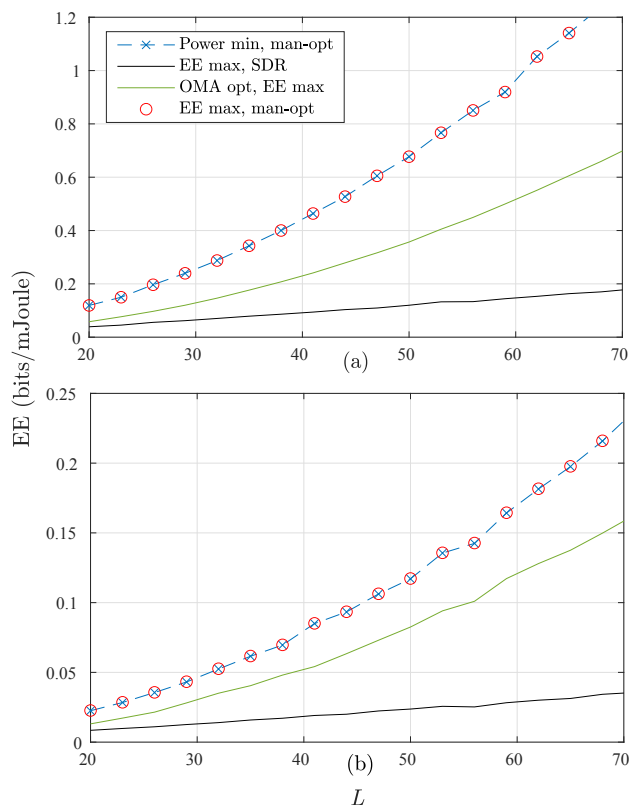


Figure 7: EE vs. number of reflectors L for high rate (a) 2-users cluster, (b) 3-users cluster

The graph shows that, in the case of high rate constraints, the sum power curve resulting from solving the EE maximization problem exactly co-insides with the sum power curve resulting from solving the total transmit power minimization problem. The rationale behind this behaviour is that the NOMA EE objective function in (37a) is pseudo concave in the transmit power vector \mathbf{p} . Hence, when the target uplink rate constraints are high, the minimum transmit powers of the users must be high too which makes it beyond the maximum EE point. Therefore, in the case of high rate constraints, moving towards the maximum EE point of the system requires decreasing the transmit powers of the users. Hence, maximizing EE in this case directly leads to minimizing the total transmit power of the users making both solutions co-inside.

Fig. 7 shows the performance comparison between the proposed EE maximization solutions using the alternation maximization scheme discussed in Sec. IV for the case of high uplink rate requirements at the users. Similar to the case of low rate constraints at the users, the figure shows a huge performance gain of the obtained EE using manifold optimization over the obtained EE using SDR. We can also notice from Fig. 7 that the EE resulted from minimizing the total transmit power by solving problem (8) is exactly the same as the EE resulted from maximizing the EE of the system by solving problem (36). This notice agrees and supports the results and discussion of Fig. 6 since we found that the EE maximization problem co-insides with the total transmit power minimization. Therefore, it is expected that the two problems

lead to the same EE values in the case of high uplink rate requirements for the users.

VII. CONCLUSIONS

In this article, we proposed efficient solutions to the sum power minimization and the EE maximization problems for the IRS assisted uplink NOMA network. The two problems are solved by jointly optimizing the users' uplink transmit powers and the IRS passive beamforming coefficients using alternation optimization based algorithms. During the passive beamforming sub-problem, we showed that the proposed manifold optimization-based solutions have significant performance gains and are far superior to the SDR based benchmark solutions. Additionally, we compared our solutions to the IRS-assisted NOMA system to the IRS-assisted OMA counterpart. The results concluded that IRS-NOMA system outperforms the IRS-OMA system only when the users' uplink minimum rate constraints are relatively high. However, the IRS-OMA system is preferable over the IRS-NOMA when the minimum required uplink rates are relatively low.

ACKNOWLEDGEMENT

This work was supported by the European Union's Horizon 2020 Research and Innovation Program through the Marie Skłodowska-Curie under grant agreement number 812991.

REFERENCES

- [1] M. A. ElMossallamy, H. Zhang, L. Song, K. G. Seddik, Z. Han, and G. Y. Li, "Reconfigurable intelligent surfaces for wireless communications: Principles, challenges, and opportunities," *IEEE Trans. Cognitive Commun. Netw.*, vol. 6, no. 3, pp. 990–1002, 2020.
- [2] E. Basar, M. Di Renzo, J. De Rosny, M. Debbah, M.-S. Alouini, and R. Zhang, "Wireless communications through reconfigurable intelligent surfaces," *IEEE Access*, vol. 7, pp. 116753–116773, 2019.
- [3] M. Di Renzo, M. Debbah, D.-T. Phan-Huy, A. Zappone, M.-S. Alouini, C. Yuen, V. Sciancalepore, G. C. Alexandropoulos, J. Hoydis, H. Gacanin, J. de Rosny, A. Bounceur, G. Lerosey, and M. Fink, "Smart radio environments empowered by reconfigurable AI meta-surfaces: An idea whose time has come," *EURASIP J. Wireless Commun. Netw.*, 2019.
- [4] Y.-C. Liang, R. Long, Q. Zhang, J. Chen, H. V. Cheng, and H. Guo, "Large intelligent surface/antennas (LISA): Making reflective radios smart," *J. Commun. Inf. Netw.*, vol. 4, no. 2, pp. 40–50, 2019.
- [5] Q. Wu, S. Zhang, B. Zheng, C. You, and R. Zhang, "Intelligent reflecting surface-aided wireless communications: A tutorial," *IEEE Trans. Commun.*, vol. 69, no. 5, pp. 3313–3351, 2021.
- [6] Y. Liu, Z. Qin, M. Elkashlan, Z. Ding, A. Nallanathan, and L. Hanzo, "Non-orthogonal multiple access for 5G and beyond," *Proc. IEEE*, vol. 105, no. 12, pp. 2347–2381, 2017.
- [7] Y. Cai, Z. Qin, F. Cui, G. Y. Li, and J. A. McCann, "Modulation and multiple access for 5G networks," *IEEE Commun. Surv. Tutor.*, vol. 20, no. 1, pp. 629–646, 2018.
- [8] Z. Ding, Y. Liu, J. Choi, Q. Sun, M. Elkashlan, I. Chih-Lin, and H. V. Poor, "Application of non-orthogonal multiple access in LTE and 5G networks," *IEEE Commun. Mag.*, vol. 55, no. 2, pp. 185–191, 2017.
- [9] Y. Liu, H. Xing, C. Pan, A. Nallanathan, M. Elkashlan, and L. Hanzo, "Multiple-antenna-assisted non-orthogonal multiple access," *IEEE Wireless Commun.*, vol. 25, no. 2, pp. 17–23, 2018.
- [10] Z. Chen, Z. Ding, X. Dai, and R. Zhang, "An optimization perspective of the superiority of NOMA compared to conventional OMA," *IEEE Trans. Signal Process.*, vol. 65, no. 19, pp. 5191–5202, 2017.
- [11] Q. Wu and R. Zhang, "Intelligent reflecting surface enhanced wireless network via joint active and passive beamforming," *IEEE Trans. Wireless Commun.*, vol. 18, no. 11, pp. 5394–5409, 2019.
- [12] C. Huang, A. Zappone, G. C. Alexandropoulos, M. Debbah, and C. Yuen, "Reconfigurable intelligent surfaces for energy efficiency in wireless communication," *IEEE Trans. Wireless Commun.*, vol. 18, no. 8, pp. 4157–4170, 2019.

- [13] Q. Wu, X. Guan, and R. Zhang, "Intelligent reflecting surface-aided wireless energy and information transmission: An overview," *Proceedings of the IEEE*, vol. 110, no. 1, pp. 150–170, 2022.
- [14] C. Pan, H. Ren, K. Wang, M. ElKashlan, A. Nallanathan, J. Wang, and L. Hanzo, "Intelligent reflecting surface aided MIMO broadcasting for simultaneous wireless information and power transfer," *IEEE J. Sel. Areas Commun.*, vol. 38, no. 8, pp. 1719–1734, 2020.
- [15] C. Huang, R. Mo, and C. Yuen, "Reconfigurable intelligent surface assisted multiuser MISO systems exploiting deep reinforcement learning," *IEEE J. Sel. Areas Commun.*, vol. 38, no. 8, pp. 1839–1850, 2020.
- [16] M. A. ElMossallamy, H. Zhang, R. Sultan, K. G. Seddik, L. Song, G. Y. Li, and Z. Han, "On spatial multiplexing using reconfigurable intelligent surfaces," *IEEE Wireless Commun. Lett.*, vol. 10, no. 2, pp. 226–230, 2021.
- [17] M. Al-Jarrah, E. Alsusa, A. Al-Dweik, and D. K. C. So, "Capacity analysis of IRS-based UAV communications with imperfect phase compensation," *IEEE Wireless Commun. Lett.*, vol. 10, no. 7, pp. 1479–1483, 2021.
- [18] X. Zhou, S. Yan, Q. Wu, F. Shu, and D. W. K. Ng, "Intelligent reflecting surface (IRS)-aided covert wireless communications with delay constraint," *IEEE Trans. Wireless Commun.*, vol. 21, no. 1, pp. 532–547, 2022.
- [19] M. Alaaeldin, E. A. Alsusa, and K. G. Seddik, "IRS-assisted physical layer network coding over two-way relay fading channels," *IEEE Trans. Veh. Technol.*, pp. 1–1, 2022.
- [20] M. A. Al-Jarrah, E. Alsusa, A. Al-Dweik, and M.-S. Alouini, "Performance analysis of wireless mesh backhauling using intelligent reflecting surfaces," *IEEE Trans. Wireless Commun.*, vol. 20, no. 6, pp. 3597–3610, 2021.
- [21] C. Pan, H. Ren, K. Wang, J. F. Kolb, M. ElKashlan, M. Chen, M. Di Renzo, Y. Hao, J. Wang, A. L. Swindlehurst, X. You, and L. Hanzo, "Reconfigurable intelligent surfaces for 6G systems: Principles, applications, and research directions," *IEEE Commun. Mag.*, vol. 59, no. 6, pp. 14–20, 2021.
- [22] Z. Ding and H. Vincent Poor, "A simple design of irts-noma transmission," *IEEE Commun. Lett.*, vol. 24, no. 5, pp. 1119–1123, 2020.
- [23] T. Hou, Y. Liu, Z. Song, X. Sun, Y. Chen, and L. Hanzo, "Reconfigurable intelligent surface aided NOMA networks," *IEEE J. Sel. Areas Commun.*, vol. 38, no. 11, pp. 2575–2588, 2020.
- [24] G. Yang, X. Xu, and Y.-C. Liang, "Intelligent reflecting surface assisted non-orthogonal multiple access," in *2020 IEEE Wireless Commun. Netw. Conf. (WCNC)*, 2020, pp. 1–6.
- [25] X. Mu, Y. Liu, L. Guo, J. Lin, and N. Al-Dhahir, "Exploiting intelligent reflecting surfaces in NOMA networks: Joint beamforming optimization," *IEEE Trans. Wireless Commun.*, vol. 19, no. 10, pp. 6884–6898, 2020.
- [26] F. Fang, Y. Xu, Q.-V. Pham, and Z. Ding, "Energy-efficient design of IRS-NOMA networks," *IEEE Trans. Veh. Technol.*, vol. 69, no. 11, pp. 14 088–14 092, 2020.
- [27] L. Bariah, S. Muhaidat, P. C. Sofotasios, F. E. Bouanani, O. A. Dobre, and W. Hamouda, "Large intelligent surface-assisted non-orthogonal multiple access for 6G networks: Performance analysis," *IEEE Internet Things J.*, vol. 8, no. 7, pp. 5129–5140, 2021.
- [28] A. S. de Sena, P. H. J. Nardelli, D. B. da Costa, F. R. M. Lima, L. Yang, P. Popovski, Z. Ding, and C. B. Papadias, "IRS-assisted massive MIMO-NOMA networks: Exploiting wave polarization," *IEEE Trans. Wireless Commun.*, vol. 20, no. 11, pp. 7166–7183, 2021.
- [29] W. Wang, X. Liu, J. Tang, N. Zhao, Y. Chen, Z. Ding, and X. Wang, "Beamforming and jamming optimization for IRS-aided secure NOMA networks," *IEEE Trans. Wireless Commun.*, vol. 21, no. 3, pp. 1557–1569, 2022.
- [30] M. Zeng, X. Li, G. Li, W. Hao, and O. A. Dobre, "Sum rate maximization for IRS-assisted uplink NOMA," *IEEE Commun. Lett.*, vol. 25, no. 1, pp. 234–238, 2021.
- [31] Z.-q. Luo, W.-k. Ma, A. M.-c. So, Y. Ye, and S. Zhang, "Semidefinite relaxation of quadratic optimization problems," *IEEE Signal Process. Mag.*, vol. 27, no. 3, pp. 20–34, 2010.
- [32] P.-A. Absil, R. Mahony, and R. Sepulchre, *Optimization Algorithms on Matrix Manifolds*. Princeton, NJ: Princeton University Press, 2008.
- [33] M. C. Pinar and S. A. Zenios, "On smoothing exact penalty functions for convex constrained optimization," *SIAM J. Optimization*, vol. 4, no. 3, 1994.
- [34] C. Liu and N. Boumal, "Simple algorithms for optimization on riemannian manifolds with constraints," *Appl Math Optim.*, vol. 82, no. 3, pp. 949–981, 2020.
- [35] N. Boumal, B. Mishra, P.-A. Absil, and R. Sepulchre, "Manopt, a MATLAB toolbox for optimization on manifolds," *J. Machine Learning Research*, vol. 15, no. 42, pp. 1455–1459, 2014. [Online]. Available: <https://www.manopt.org>
- [36] K. Shen and W. Yu, "Fractional programming for communication systems—part I: Power control and beamforming," *IEEE Trans. Signal Process.*, vol. 66, no. 10, pp. 2616–2630, 2018.